Copyright © 1998, by the International Council of the Aeronautical Sciences (ICAS)
and the American Institute of Aeronautics and Astronautics, Inc.

ICAS-98-1,7,4

A98-31469

HIGH ANGLES OF ATTACK FLIGHT DYNAMICS OF CONTEMPORARY AND PROSPECTIVE FIGHERS AS A FUNCTION OF THEIR CONFIGURARTION AND AERODYNAMICS

Zdobysław Goraj, Ph.D., D.Sc., Prof.
Warsaw University of Technology, Warsaw, Poland

Abstract

This paper reviews the performance of modern agile aircraft at very high incidence, near and beyond stall. Includes discussions of the research and development efforts devoted to the investigations of the numerous flight dynamic and aerodynamic phenomena that are accentuated as the angle of attack of the modern complex configurations increases beyond stall. Necessary conditions to sustain appreciable lift force at post stall conditions for special maneuvers even far beyond stall angle as demonstrated in the "Cobra Maneuver", are reviewed. A dynamic entrance into the post-stall region of angles of attack has been numerically simulated. Static aerodynamic characteristics and some dynamic stability derivatives with respect to pitch and normal acceleration, used in this paper for numerical simulation of motion in the extended range of angle of attach (from 0° to 90°), have been elaborated coming from results of wind tunnel experiments, numerical engineering methods (including panel methods) and results published by other authors. Aerodynamic hysteresis, associated lag and dependence of stability derivatives on frequency of oscillation were not included into analysis. Transient responses of an aircraft were numerically computed for different centres of mass position, tailplane control function, canard deflection etc. Trim parameters were found for steady flight at the below and post-stall regions. These parameters were computed either from the full nonlinear equations of the state of equilibrium or from simplified, two different sets of linear equations. All numerical results were obtained for a conceptual design project of an aircraft, considered as a candidate for subsonic, ground attack fighter.

Introduction

The paper discusses different aspects of the high angles of attack (AoA) flight dynamics, mainly from the point of view the relation between dynamics, control, aerodynamics and aircraft configuration. It considers pitching moment characteristics desired for a state of equilibrium. Manoeuvring at supercritical AoA, so-called super and hyper-manoeuvrability, is considered[1,2,3]. The pitching moment curves for an aircraft, which is (1) static stable, (2) neutral and (3) static unstable, all of them with the same angle of tailplane deflection are quite different. The static-stable aircraft with the tailplane setting angle being fixed has only one point of balance, whereas the static-unstable aircraft has two different points of balance[2,4,5]. It means that to be the so-called super manoeuvrable the aircraft should be static-unstable at lower AoA and static-stable at higher, post-critical AoA. It also means that the characteristic curve of pitching moment C_m versus AoA should be a non-linear one. A concentration of characteristic curves C_m for the tailplane setting angle φ_t being varied at post-critical AoA (i.e. very low sensitivity of pitching moment with respect to the tailplane setting angle) reflects the loss of effectiveness of a horizontal tail at higher AoA. For super manoeuvre aircraft the return back from the high AoA to the initial flight condition should be possible independently of the effectiveness of the tail control surfaces[6]. An increasing of the initial measure of instability (for $\alpha \cong 0$) above an optimal one results in an increased AoA at which equilibrium is possible, however this also means that the equilibrium will be kept at the AoA, close to the critical angle, and leads to the lack of pitching moment for diving in the range of moderate AoA. It can result in the stoppage of the aircraft at this range of AoA and an impossibility to fly at high AoA at all. To fly safely at high AoA without a complicated AFCS it is necessary to have for the point of maximum pitching moment coefficient C_m, corresponding to the maximum deflection of the tailplane for diving, a margin of pitching moment coefficient, equal at least 0.05. At higher AoA ($\alpha \geq 30°$) vortices breaks-down and lifting characteristics become worse[7,8,9,10,11]. The existence of LEXes increases the requirements for the design of horizontal tailplanes[12,13]. This is because the downwash field at moderate and high AoA is strongly unequal. Above of the wing chord plane there is the maximum downwash region. It is the result of a displacement of the vortex from the LEX root - this vortex breaks-down behind the wing. The maximum downwash corresponds to its unpleasant influence on the AoA (i.e. with the increasing of derivative $\partial\varepsilon/\partial\alpha$). Below the wing chord plane the downwash field in the vicinity of the horizontal tailplane is much more uniform. A tail ahead of the main wing either in Canard or three-wing configuration in a subsonic range of speed takes the role of a LEX and increases the lifting force coefficient at AoA. However, a LEX is much more effective - with respect to the unit of the flow-round surface - in the sense of the increase of the lifting force coefficient[14]. It is due to the sweep angle of the leading edge and the strength of the shedding-down vortices - the greater sweep angle of a LEX generates stronger vortices and a higher lifting force coefficient[15]. Therefore, the unbalanced maximum lifting force coefficient for a conventional aircraft configuration

Copyright © 1998 by ICAS and AIAA. All rights reserved

Copyright © 1998, by the International Council of the Aeronautical Sciences (ICAS)
and the American Institute of Aeronautics and Astronautics, Inc.

with a LEX is a little bit higher than that of the Canard configuration[16,17,18,19,20]. However, if the flight is in equilibrium conditions, the Canard configuration is able to deliver the higher lifting force and a sufficiently efficient control surface for longitudinal control. Moreover, because the span of canard is greater than that of the LEX, therefore the vortices shedding-down from the front wing increase the lifting characteristics of the outer parts of the main wing and change the characteristics of lateral stability for the better.

Many papers devoted to analysis, synthesis and optimization of aircraft manoeuvres were published. Lately even academic books contain chapters describing classical and modern, post-stall manoeuvres[21]. Some papers are devoted to both dynamics and aerodynamics aspects of high angles of attack[22,23,24,25,26,27,28,29], others are limited to pure aerodynamic considerations[30,31,32,33,34,35,36,37], because it seems that just the quality and accuracy of aerodynamic characteristics decide about the success of post-stall manoeuvre analysis. Another important feature in the combat effectiveness of post-stall manoeuvre is design layout of the aircraft[28,38,39]. Two-surface or three-surface configuration and an influence of many design parameters on aircraft performances, induced drag and various dynamic characteristics were analysed in[40].

All above-mentioned phenomena, known from wind-tunnel and flight tests, are numerically simulated in the present paper. A dynamic model of symmetrical motion has been developed and investigated for various aerodynamic, mass and geometry characteristics. Some numerical results were obtained for conceptual project of a ground-attack aircraft.

Flight Dynamics at High Angles of Attack

According to the new concept of air fighting, manoeuvring should enable the aircraft to „catch" an enemy aircraft in its sphere of successful shooting, being itself out of the successful shooting sphere of the enemy aircraft. It can be achieved due to extending the range of angles of attack and sustained manoeuvring at flight speed higher than that of the enemy aircraft.

Flying at high angles of attack may result in some adverse effects, such as the wing-rock, tail-buffet, nose-slice or spin departure phenomena. The manoeuvres may be restricted by the inefficiency of the available control surfaces, causing insufficient pitching moment or inadequate roll response. Let us look at the aerodynamics of high-alpha manoeuvres and start from the steady flight under these conditions. The flow around an aircraft is largely separated, unsteady and contains one or more vortex systems, shedding from forebody and leading, side and trailing edges. As the angle of attack increases, these vortices can become asymmetric, even though the angle of sideslip remains zero. As alpha increases even further, the vortices undergo breakdown[7]. It starts somewhere in the wake and gradually moves forward towards the nose configuration. Vortex breakdown may cause major effects on the aerodynamic loads and render all aerodynamic characteristics highly nonlinear.

To summarise flow phenomena, characteristic for moderate and high angles of attack, we emphasise the important features, different from that of known in the small angles of attack:

- ad. moderate angles: some flow asymmetries; small time lags; moderate non-linearities; extended stability derivatives (which are functions of flight variables and include cross-coupling), see Orlik-Rückemann [23,24,25]
- ad. high angles: moderate flow asymmetries; significant time lags; large non-linearities (stability derivatives do not have sense and a new representation of dynamics is needed)[29].

Super and hyper-manoeuvrability

At subsonic speeds the manoeuvring at supercritical angles of attack can be realised in two different flight conditions[1,2]. These states of flight are referred to as:

- **Super-manoeuvrability (SM)** - if the aircraft can fly at angles of attack of 60° - 70° with the ability for control in all channels;
- **Hyper-manoeuvrability (HM)** - if the aircraft can fly at angles of attack of 80° - 120° with the ability to maintain stability in all channels. In this flight regime the ability for conventional control is usually lost.

In this sense **hyper-manoeuvrability (HM)** can be considered as the flight regime where the dynamic entrance into supercritical angles of attack is possible. It must be emphasised that **SM** mode does permit a decrease in the space of steady turn in 2 - 2.5 times. An **SM** regime can be achieved by some aircraft of the fourth generation, i.e. by Su-27, MiG-29, F-15, F-16, F-18, and an **HM** regime can be achieved by the Su-27, Su-37 and F-22.

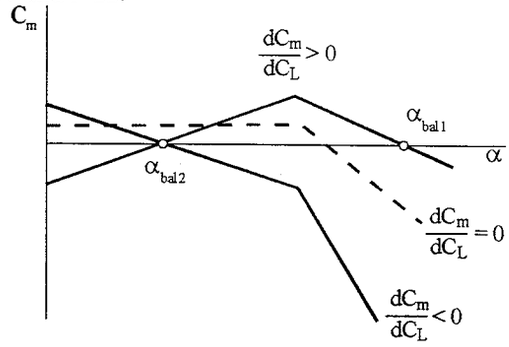

Fig. 1. Qualitative characteristics of the pitching moment for static stable, neutral and unstable aircraft[1]

Requirements for pitching moment characteristic

The necessary condition to fulfil either an **SM** or **HM** regime of flight is the possibility to reach an angle of

Copyright © 1998, by the International Council of the Aeronautical Sciences (ICAS)
and the American Institute of Aeronautics and Astronautics, Inc.

attack higher than 60°. For this aim the aircraft flying at supercritical angles of attack (higher than 30°) should :

- have a state of equilibrium at high angles of attack
- possess a sufficient margin of pitching moment for recovery into the level, steady flight[2].

Fig.1 shows qualitative characteristics of the pitching moment C_m for an aircraft, which is (1) static stable, (2) neutral and (3) static unstable, all of them with the same angle of tailplane deflection. Curves at Fig.1,2 show the fundamental difference between the balance of static-stable and unstable aircraft. The static-stable aircraft with the tail setting angle φ_t = const has only one point of balance α_{bal}, whereas the static-unstable aircraft for φ_t = const has two different points of balance α_{bal}. It means that to realise either an **SM** or **HM** regime of flight the aircraft should be static-unstable at lower angles of attack and should be stable at higher, post-critical angles of attack.

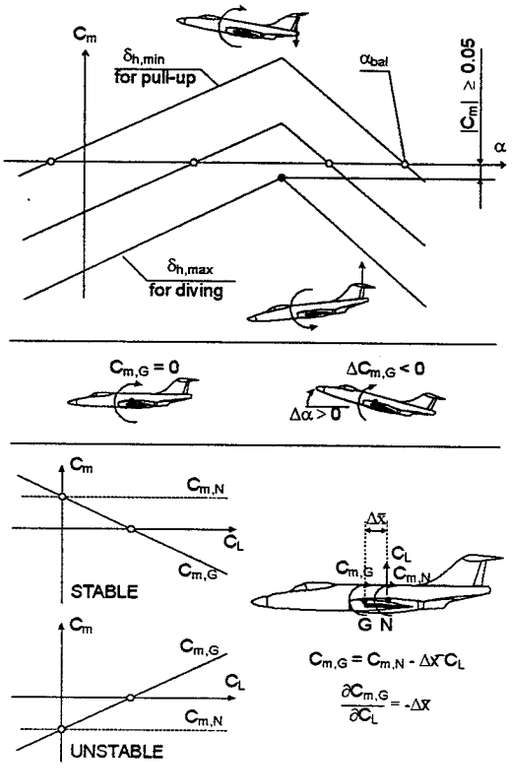

Fig.2 Theoretical dependence of pitching moment coefficient on deflection of horizontal tail (top) and relations between the moment point of reference, moment curve-slope and stability (bottom)

Presented in Fig.3 are two typical forms of pitching moments C_m (α, φ_t) for an aircraft of the Canard configuration. The curves (from top to bottom) correspond to the different margins of static, longitudinal stability (from the unstable aircraft ($\partial C_m / \partial C_L$ = -0.05) to the stable one ($\partial C_m / \partial C_L$ = 0.05)).

Calculation methods for the aerodynamic characteristics of configurations at high angles of attack[3,4]

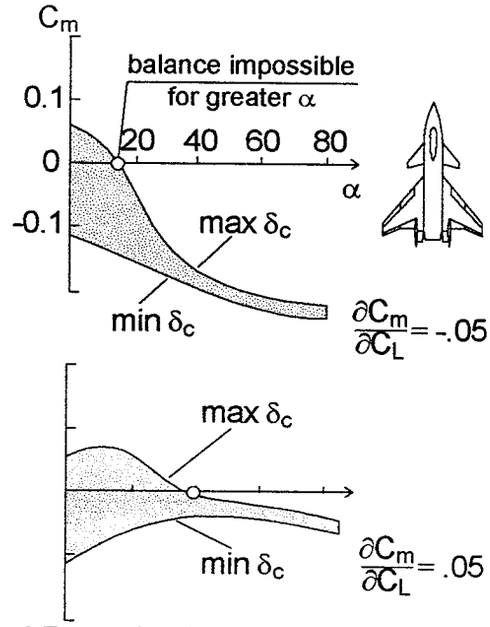

Fig.3 Forms of pitching moments for classical and Canard configurations (adopted from[2])

The aerodynamics of complex configurations is determined by the three-dimensional separated flows. The separated viscous layers roll up into vortex structures that dominate the flow over the configuration. It is the separated viscous layers that establish the rolled-up vortices, but once these vortices are free, their induced flow is approximately the same as that induced by inviscid vortices. It is therefore possible to use solutions of the inviscid equations as reasonable approximation for the calculations of the aerodynamic characteristics of the configuration up to high angles of attack. This is the reason that reasonable results are obtained, for certain aerodynamic coefficients at low and moderate angles of attack, even with the panel methods. At higher angles of attack the nonlinear panel methods and numerical solutions of the Euler equations enable reasonable results using relatively small computer resources. The panel methods enable very fast computations so that it is possible to use them for calculations of non-steady aerodynamic phenomena. The correct calculation for the flow over complex configurations at high angles of attack requires the numerical solution of the Navier Stokes equations. Such solution of the flows over a modern aircraft configuration requires very large computer resources. Therefore, at present, most aerodynamic design is still done using various panel codes. In the more advanced design studies Euler solution codes are widely used[3,35].

Analysis of Cobra manoeuvre[41,42,43,44]

Three design characteristics are necessary the aircraft could execute dynamic entrance into Cobra manoeuvre. Firstly, a high nose-up pitch control; secondly, lateral stability and control; and thirdly a robust pitch-down

Copyright © 1998, by the International Council of the Aeronautical Sciences (ICAS)
and the American Institute of Aeronautics and Astronautics, Inc.

recovery. The trim requirements at supersonic speeds usually result in an excess nose-up control power at subsonic speeds. Also an increased negative static margin at subsonic speeds and mechanism of vortex lift enhance high nose-up pitch control. The pitch motion is highly dynamic (with the acquired kinetic energy of pitch) allowing the aircraft to overshoot its trim angle of attack at post-stall region. The provision of high lateral stability, especially at angles of attack about 30°, is sometimes referred as a „black art"[6], and the only way to overcome this instability is to cross it in a reduced time before passing into the fully separated flow at higher angles of attack. The recovery from high angles of attack to the classical flight mode in a few seconds only is possible due to moving the centre of pressure on main wing back and creating the strong nose-down aerodynamic pitching moment about centre of gravity. This nose-down pitching moment arrests the positive pitch motion and starts recovery to previous flight conditions. By the time the pre-manoeuvre flight is re-established the full afterburner mode is necessary to regain lost speed. For more details see[2,6].

Dynamic equations of motion

Dynamic, nonlinear equations of motion for aircraft of three degrees of freedom have been written in the body axis system. The origin of the axis system coincides with the mean wing quarter-chord point, Ax_A axis is directed forward of the aircraft along the mean aerodynamic chord, Az_A axis is perpendicular to Ax_A and is directed downward. These equations have the form:

$$m(\dot{U}+QW)-mz_c\dot{Q}+mx_cQ^2=X(\alpha,Q,\dot{w})-mg\sin\theta, \quad (1)$$

$$m(\dot{W}+QU)+mx_c\dot{Q}+mz_cQ^2=Z(\alpha,Q,\dot{w})+mg\cos\theta, \quad (2)$$

$$J_y\dot{Q}+mx_c\dot{W}-mx_cUQ-mz_c\dot{U}-mz_cQW=M_A(\alpha,Q,\dot{w})+mgz_c\sin\theta+mgx_c\cos\theta, \quad (3)$$

where U, W are velocity components in the body frame of reference, Q - angular velocity, Θ - pitch angle, M_A - pitching moment about the mean quarter-chord point (1/4 MAC point), x_c, z_c - mass centre coordinates in the body frame of reference, $\dot{w}$ - acceleration along Az axis. Aerodynamic forces X,Z and pitching moment M_A depend on angle of attack α, pitch rate Q and acceleration $\dot{w}$.

Aerodynamic characteristics

Classical stability derivatives widely used in flight dynamics can not be applied here to compute forces and moment. It is because that in extreme manoeuvres (as in Cobra manoeuvre for example) all flight parameters change rapidly and usually are highly distinct from that of in the steady flight. There are two possibilities to tackle this problem in order to obtain the time-dependent aerodynamic forces - problem which is the key point in numerical simulation of any extreme manoeuvre. One possible way is to solve synchronously the fluid dynamic equations (for example Navier-Stokes equations) using a selected CFD code together with flight dynamic equations of motion. However according to the author's best knowledge a practical utilisation of CFD in the most general case of an arbitrary configuration, being in an arbitrary motion is still impossible and beyond the power of to-day computers. The other possible approach is to use the time-depend forces and moments, known in the whole range of angle of attack and being the functions of Mach number, Reynolds number, pitch rate, reduced frequency and normal acceleration. Such functions should be measured in wind tunnel tests, so they are very costly to obtain and need highly specialized laboratory equipment[45,46]. An example of so-called „reaction surfaces" is presented by Rückemann[29]. Aerodynamic data used in this paper for numerical simulation were partially computed (in linear range), partially measured in wind tunnel and partially estimated (interpolated or extrapolated) on the base of results obtained by other authors[45,46]. Coefficients and derivatives used in farther analysis were defined as follows:

$C_N=\frac{F_N}{q_\infty S}$ - normal force coefficient ($F_N = -Z$),

$C_A=\frac{F_A}{q_\infty S}$ - axial force coefficient ($F_A = -X$),

$C_D=\frac{F_D}{q_\infty S}$ - drag coefficient (where $F_D = D = F_A\cos\alpha + F_N\sin\alpha$),

$C_m=\frac{M_A}{q_\infty S c_a}$ -pitching moment coefficient,

$C_{Nq}=\frac{\partial C_N}{\partial\frac{qc_a}{V}}$ - normal force derivative with respect to pitch rate,

$C_{Aq}=\frac{\partial C_A}{\partial\frac{qc_a}{V}}$ - axial force derivative with respect to pitch rate,

$C_{mq}=\frac{\partial C_m}{\partial\frac{qc_a}{V}}$ - pitching moment derivative with respect to pitch rate,

Copyright © 1998, by the International Council of the Aeronautical Sciences (ICAS)
and the American Institute of Aeronautics and Astronautics, Inc.

$C_{N\dot{\alpha}} = \frac{\partial C_N}{\partial \frac{\dot{\alpha} c_a}{V}}$ - normal force derivative with respect to normal acceleration

$C_{A\dot{\alpha}} = \frac{\partial C_A}{\partial \frac{\dot{\alpha} c_a}{V}}$ - normal force derivative with respect to normal acceleration

$C_{m\dot{\alpha}} = \frac{\partial C_m}{\partial \frac{\dot{\alpha} c_a}{V}}$ - pitching moment derivative with respect to normal acceleration.

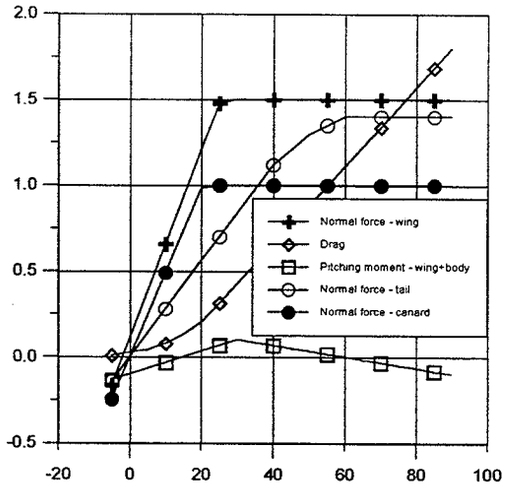

Fig.4 Aerodynamic characteristics as the functions of angle of attack in the range of -5° to 90°

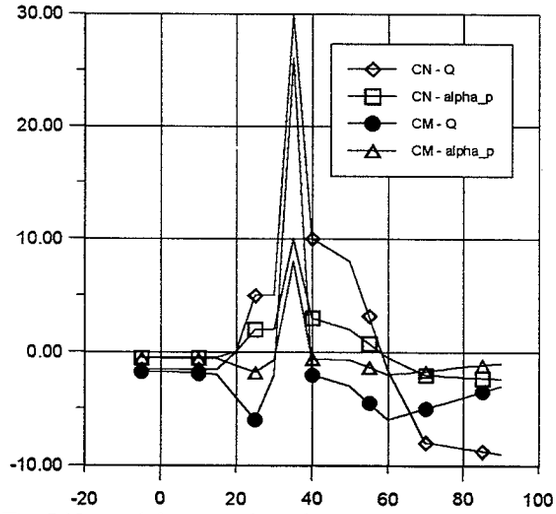

Fig.5 Normal force and pitching moment derivatives (excluding contribution of canard and horizontal tail) with respect to pitch rate and normal acceleration

Both the static and dynamic pitching moment data are referred to a mass center located at 25 % of MAC. The configuration under consideration appeared to be statically unstable (neutral point of maneuverability was located at 13 % of MAC). Important aerodynamic characteristics are presented in Fig.4-6. Normal force coefficients on all control surfaces (i.e. on main wing: C_{Nw}, on canard: C_{NC} and on horizontal tail: C_{NH}) reach their maximums and keep it in the whole post-stall region of local angles of attack. Axial force at high angle of attack is much lower than the normal force and was even neglected (at the first approximation) in the case of canard and horizontal tail. However, if we look at lift and drag coefficients (lift is not shown here), we could see that lifting force decreases to zero and drag coefficient is extremely high and keeps almost constant as angle of attack goes to 90°. Normal force and pitching moment strongly depend on pitch rate and normal acceleration.

Presented data show that the configuration has stable values of damping both pitch and plunge (negative values of C_{mq} and $C_{m\dot{\alpha}}$) over most of the angle of attack range. However, large reduction in damping occurs near lift maximum (when α = 30°). Grafton[46] explains this phenomenon, displayed also by other airplanes, as being involved by the same mechanism as that producing stall flutter. This instability is related to hysteresis and associated lag of the flow during oscillatory motion when flow separation exists. Downwash field at moderate and high angles of attack is strongly unequal, Fig.6. Above of the wing chord plane there is usually the maximum downwash region. It is the result of a displacement of the vortices created on LEX's and canard control surface. These vortices break-down behind the wing and strongly influence the downwash field. Fig.6 was obtained by use of panel methods and does not include the effects involved by LEX vortices. However, considered configuration has the wing and tailplane almost at the same plane, so downwash distribution approximated by use of panel method and shown in Fig.6, can be regarded as of sufficient accuracy.

Configuration being considered in this paper is shown in Fig.7. It is one of many variants analysed and considered for subsonic, ground-attack fighter. Aircraft was planned to be equipped with a four-channel, digital FBW flight control system. The agility, survivability and low-speed manoeuvrability were required as the goals of primary importance.

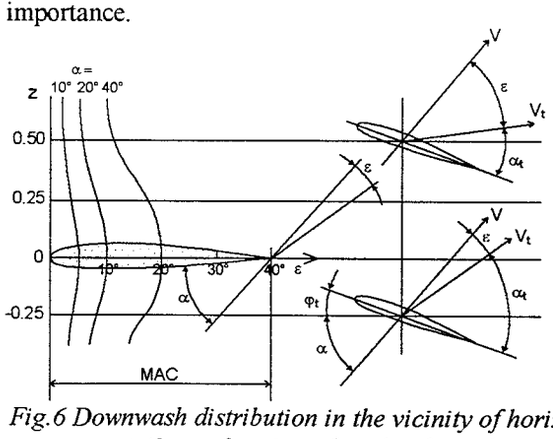

Fig.6 Downwash distribution in the vicinity of horizontal tail as a function of angle of attack

Copyright © 1998, by the International Council of the Aeronautical Sciences (ICAS)
and the American Institute of Aeronautics and Astronautics, Inc.

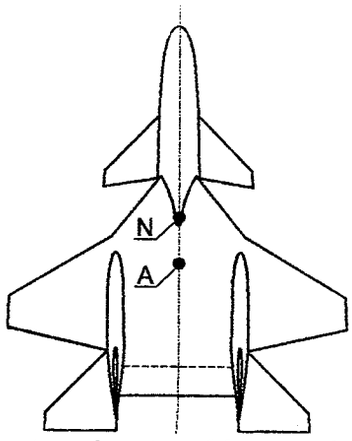

Fig.7 Plan view of an aircraft being analysed in this paper. A - mean quarter-chord point (25 % of MAC); N - neutral point of stability (13 % of MAC)

Analysis of maneuvers was preceded by solving the equation of longitudinal equilibrium. These equations can be obtained from dynamic equation of motion assuming that all accelerations and angular velocities are equal to zero. Knowing[2,4] that the supermanoeuvre aircraft has to be stable at the range of high angles of attack and unstable at the range of small angles of attack one can expect that at each, prescribed speed and for assumed canard setting the aircraft has two distinct, steady flight conditions (i.e. states of trim). They are:

- small angle of attack, unstable state of trim. Flying at small angles of attack, especially at trim condition, is very well known, however for most of the aircraft this point of equilibrium is statically stable;
- high angle of attack, longitudinally stable state of trim. Only a few aircraft can fly at the „sustained" high angles of attack range, attaining the state of trim (among them are Su-27, Su-37 and Mig-29). Depending on flight condition, configuration, state of atmospheric parameters etc., this post-stall angle of trim is usually close to 60°. In fact, even for some modern fighter aircraft the so-called sustained flight is rather a theoretical possibility only, first of all because flying at high angles of attack is accompanied by strongly unstable lateral flow. However, for some fighter aircraft it is possible to find numerically two, different states of trim (for the same speed and thrust values).

In this paper the following algebraic equations of equilibrium were used (Fig.8):

$$C_{LC}\frac{S_C}{S}+C_{LN}+C_{LH}\frac{S_H}{S}-C_G\cos\Theta=0, \quad (4)$$

$$-C_A+C_F-C_G\sin\Theta+C_{AC}\frac{S_C}{S}+C_{AH}\frac{S_H}{S}=0, \quad (5)$$

$$C_{LC}k_C+C_G\bar{x}_C\ Q+C_{m,W+B}-C_{LH}k_H=0, \quad (6)$$

where

$C_G=\frac{G}{qS}$; $C_F=\frac{F}{qS}$ are weight and thrust coefficients;

$\kappa_C=\frac{S_C x_C}{S c_a}$; $\kappa_H=\frac{S_H x_H}{S c_a}$ are canard volume or horizontal tail volume, respectively;

$\Theta=\gamma+\alpha$ - pitch angle;

$C_{m,W+B}$ - wing-body pitching moment coefficient,

$q = 1/2\ \rho V^2$ - dynamic pressure.

To solve this equations the following parameters have been used:

$x_C = 3.9$ m, $x_H = 3.7$ m , $m = 4900$ kg , $S_C = 5.7$ m^2, $S_H = 3.3$ m^2, $S = 33$ m^2, $\rho = 1.225$ kg/m^3, $V = 40 \div 120$ m/s; $a_W = 0.0548$ 1/deg; $a_C = 0.0487$ 1/deg; $a_H = 0.047$ 1/deg ; $\partial C_{m,W+B}/\partial\alpha = 0.00667$.

Gradients a_W, a_C, a_H, $\partial C_{m,W+B}/\partial\alpha$ were used for the range of small angles of attack - for higher angles of attack the full, nonlinear aerodynamic functions have to be used (Fig.4-6).

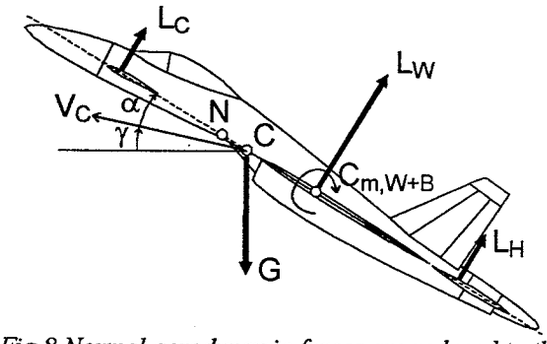

Fig.8 Normal aerodynamic forces are reduced to the mean quarter-chord points of the local lifting surfaces

State of equilibrium - small angles of attack

Assume that angle of attack on main wing, canard and horizontal tail is small, i.e. that aircraft operate in the linear range of normal forces. In this case the aerodynamic characteristics can be expressed as follows:

$$C_C = a_C(\alpha+\delta_C); \quad (7)$$

$$C_H = a_H\alpha(1-\partial\varepsilon/\partial\alpha)+\delta_C; \quad (8)$$

$$C_W = a_W\alpha; \quad (9)$$

$$C_{W+B} = C_{W+B,0}+\partial C_{W+B}/\partial\alpha\ \alpha. \quad (10)$$

These assumptions allow to simplify equations (2-3) . They take the form of linear equations:

$$\mathbf{A}\,\mathbf{X}=\mathbf{B}, \quad (11)$$

where

$$X(1)=\alpha\ ,\ X(2)=\delta_H, \quad (12)$$

$$A(1,1)=a_W+a_H\left(1-\frac{\partial\varepsilon}{\partial\alpha}\right)\frac{S_H}{S}+a_C\frac{S_C}{S}, \quad (13)$$

$$A(1,2)=a_H\frac{S_C}{S}\ ;\ A(2,2)=-a_H\kappa_H, \quad (14)$$

Copyright © 1998, by the International Council of the Aeronautical Sciences (ICAS)
and the American Institute of Aeronautics and Astronautics, Inc.

$$A(2,1)=\frac{\partial C_{m,W+B}}{\partial\alpha}-a_H\left(1-\frac{\partial\varepsilon}{\partial\alpha}\right)\kappa_H+a_C\kappa_C\,, \quad (15)$$

$$B(1)=C_G-a_C\frac{S_C}{S}d_C\,, \quad (16)$$

$$B(2)=-C_{m,W+B,0}-C_G\bar{x}_G-a_C\kappa_H\delta_C\,. \quad (17)$$

Assuming that we know speed, flight angle and setting of canard surface we can use eq.(11-17) to find angle of attack and horizontal tail deflection.

State of equilibrium - post-stall angles of attack

Assume that angle of attack is sufficiently high that normal force coefficients on main wing and canard have their maximum values. Because of very strong downwash there is still a chance to have moderate angle of attack in the vicinity of horizontal stabilizer (assuming that angle of attack on main wing is not greater than 70° and that horizontal elevator is deflected up, i.e. elevator trailing edge is moved up). So, lifting force coefficient on horizontal elevator can be computed using eq.(8). Eq.(4-6) were rewritten as follows:

$$C_{NC,\max}\frac{S_C}{S}+C_{NW,\max}+a_H(\alpha-\varepsilon+\delta_H)\frac{S_H}{S}-C_G\cos\Theta=0\,, \quad (18)$$

$$C_{NC,\max}\kappa_H+C_G\bar{x}_G\cos\Theta+C_{m,W+B}(\alpha)-a_H(\alpha-\varepsilon+\delta_H)\kappa_H=0\,. \quad (19)$$

They also have the form of linear equations and can be written in form of (11), where

$$A(1,1)=a_H\frac{S_H}{S}\;;\;A(1,2)=-\cos\Theta\;;\quad A(2,1)=-a_H\kappa_H\;;\;A(2,2)=\bar{x}_G\cos\Theta\;; \quad (20)$$

$$B(1)=C_{NC,\max}\frac{S_C}{S}+C_{NW,\max}+a_H(\alpha-\varepsilon)\,, \quad (21)$$

$$B(2)=C_{NC}\kappa_H+C_{m,W+B}-a_H(\alpha-\varepsilon)\kappa_H\,, \quad (22)$$

$$X(1)=\delta_H\;;\;X(2)=c_G\,, \quad (23)$$

$$v=\sqrt{\frac{2G}{\rho S C_G}}\,. \quad (24)$$

Assume that we know the values of angle of attack, path angle and setting of canard surface. Then we can use eq.(11) with coefficients (20-22) to find the horizontal tail deflection δ_H, weight coefficient C_G, and then the aircraft speed V from eq.(24).

Numerical results and recommendations

The trim conditions were found using the linear models, (eq. 11-17 or 11,20-22) and the full nonlinear equations (4-6), solved by use of the so-called hyper-tangent planes algorithm. Obtained results are very close one to the other. Important difference is that in order to find the nonlinear solution one needs the starting point has to be precisely estimated, otherwise the numerical process is divergent. Execution time in both cases is very short. Fig. 9-14 present angle of attack and tailplane deflection at extended range of velocities (corresponding to the below-stall and post-stall range of angles of attack) for various design and flight parameters (XC - position (in % of MAC) of mass centre along wing mean chord, starting from its leading edge; deltac_c - canard deflection; gamma - flight path angle). Curves of both regions are displayed with a discontinuity, corresponding to angle of attack equal to about 30° and speed range from 30 to 40 m/s. Longitudinal trim conditions could be found in this region also, however they do not have any practical importance because of the beginning of flow separation, unsteadness and lateral/directional instability. Canard deflection (delta_c) influences the angle of attack in the below-stall range, see Fig.10, and does not influence in the post-stall range. Moreover, canard deflection influences the tailplane deflection in the below-stall region only, see Fig.11, and does not influence in the post-stall one.

Angle of attack and tailplane deflection depend very strongly on the flight path angle in the post stall region and practically do not depend in the below-stall region, Fig.12-15. Trim angle of attack (alpha) and tailplane (delta_h) in the whole extended range of flight speed are given in Fig.14. Flight speed versus angle of attack for various flight path angles are shown in Fig.15. Post-stall trim conditions corresponding to these three various path angles (γ = 20°, 0, -20°) and various pitch angles (Θ = 50°, 40°, 40°) are presented in Fig.16. Important conclusion from analysis of the curves presented in Fig.9-15 is that in the post-stall region the trim angle of attack is, depending on various design parameters, equal to about 70°. Because above the post-stall trim-angle-of-attack the pitching moment coefficient (Fig.1,2) is negative and the pitching moment derivative with respect to pitch rate (Fig.5) is also negative it means that the positive pitch rate will be decelerated, then will change sign and aircraft return back to its initial, below-stall range of flight conditions.

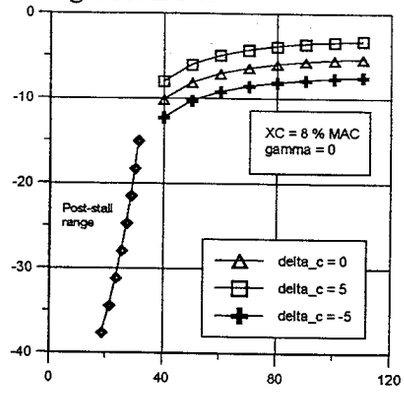

Fig.9 Deflection of horizontal tail versus speed in the extended range of angles of attack

Copyright © 1998, by the International Council of the Aeronautical Sciences (ICAS)
and the American Institute of Aeronautics and Astronautics, Inc.

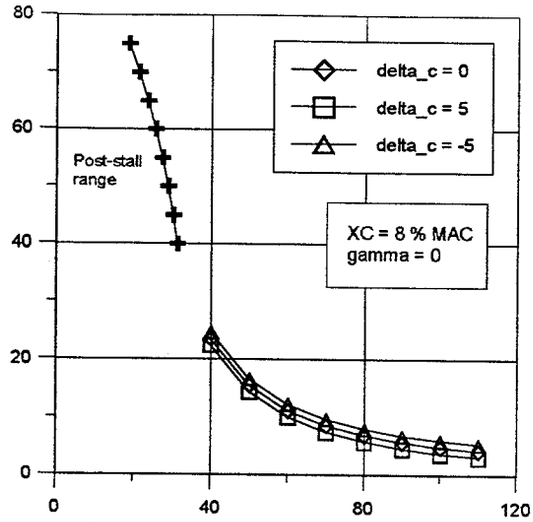

Fig.10 Angle of attack versus speed under trim condition in the extended range of flight parameters

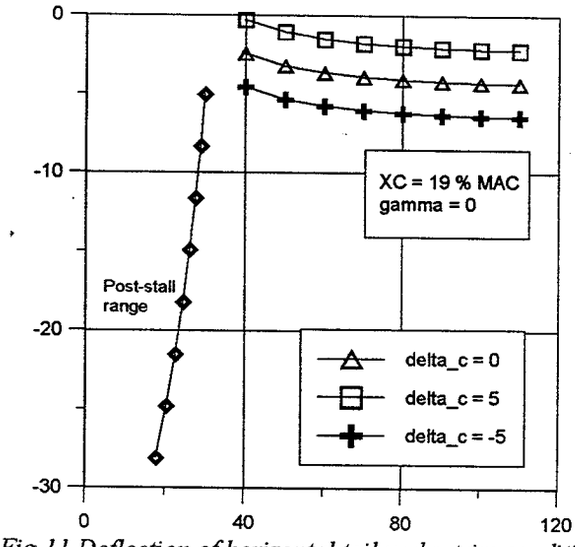

Fig.11 Deflection of horizontal tail under trim condition versus speed

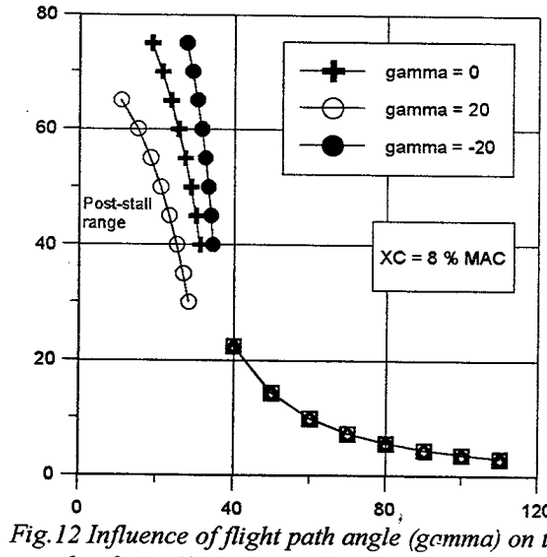

Fig.12 Influence of flight path angle (gamma) on the angle of attack versus speed under trim condition

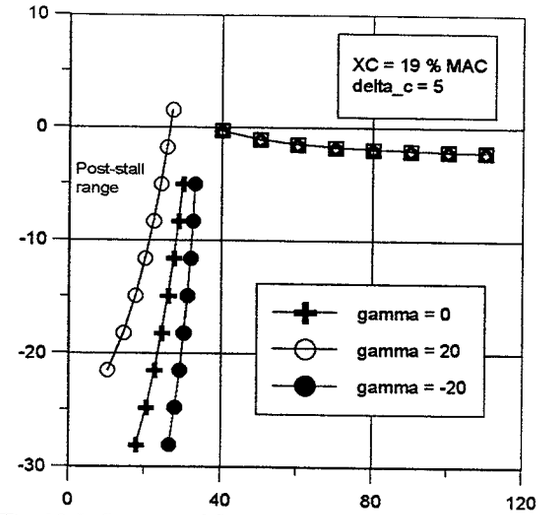

Fig.13 Influence of flight path angle (gamma) on the angle of horizontal tail deflection versus speed under trim condition

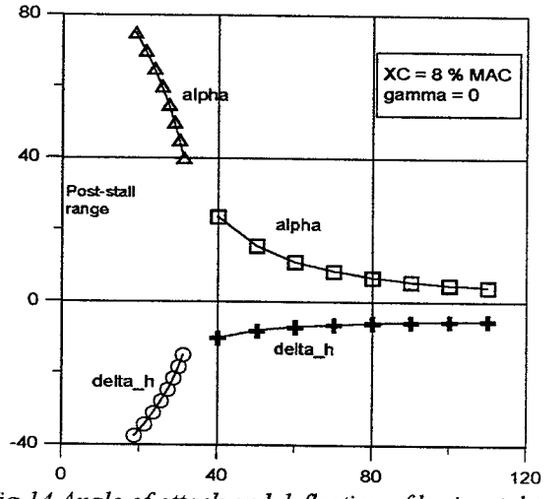

Fig.14 Angle of attack and deflection of horizontal tail versus speed under trim condition in the below-stall and post-stall regions

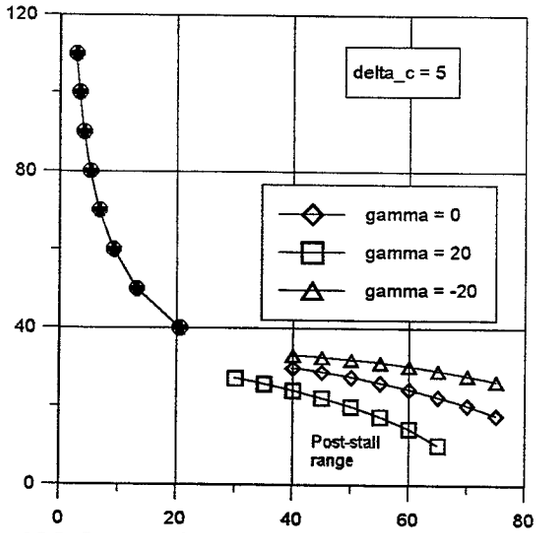

Fig.15 Influence of flight path angle (gamma) on flight speed versus angle of attack under trim condition

Copyright © 1998, by the International Council of the Aeronautical Sciences (ICAS)
and the American Institute of Aeronautics and Astronautics, Inc.

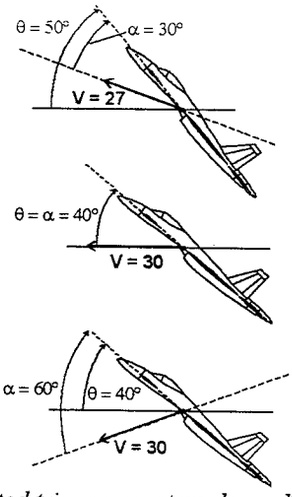

Fig.16 Selected trim parameters depending on flight path angle

Transient responses presented in Fig.18-21 were computed numerically. Dynamic equations of motion (1-3) were integrated under the assumption that tailplane was deflected according a time function shown in Fig.17. In the beginning the tailplane is deflected to a value corresponding to state of equilibrium (Fig.17), after 3 seconds is rapidly moved up (about 5 degrees in negative direction) what produces high pitch rate and creates rapid nose-up manoeuvre. After next 2 seconds tailplane deflection is increased up to -12° and then is quickly reduced to initial, trim value. Additional deflection, also in negative direction in the time interval between 7 and 8 seconds, is done to smooth the highly violent, transient response of the aircraft. Here it should be emphasised that transient responses are very sensitive to the shape of control function.

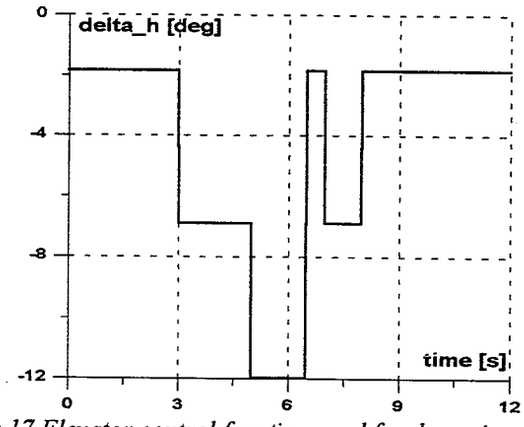

Fig.17 Elevator control function used for dynamic entrance into the post-stall region of angles of attack

Fig.18 presents flight altitude after the rapid tailplane deflection given in Fig.17. In a few time points there are drawn the aircraft silhouettes showing its current attitude (i.e. pitch angle). Flight altitude increases on about 150 m in 6 seconds time after the beginning of the manoeuvre and the pitch angle grows-up to 110° in 4 seconds time. Speed shown in Fig.20 decreases very rapidly to about 30 m/s. It is because of the enormous rise in drag - aircraft being almost perpendicular to its velocity vector - reaches drag coefficient equal to 1.6 (see Fig.4). To be able to re-establish the steady, level flight the full afterburner has to be selected to regain lost speed.

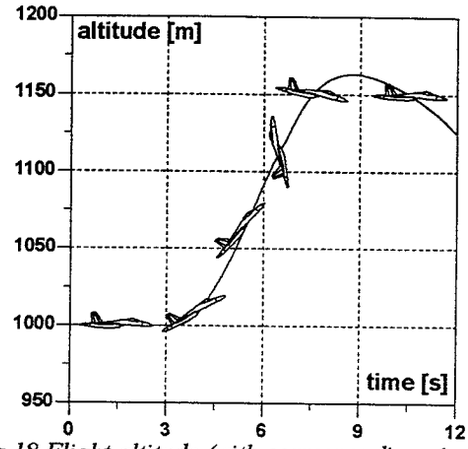

Fig.18 Flight altitude (with corresponding aircraft attitude) versus time after dynamic entrance into post-stall region of angles of attack

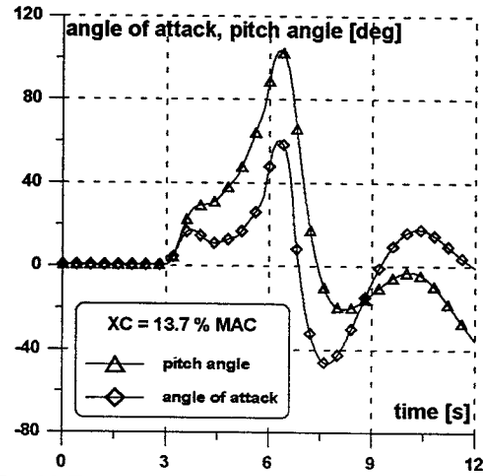

Fig.19 Transient dynamic response after a rapid entrance into the post-stall region of angles of attack

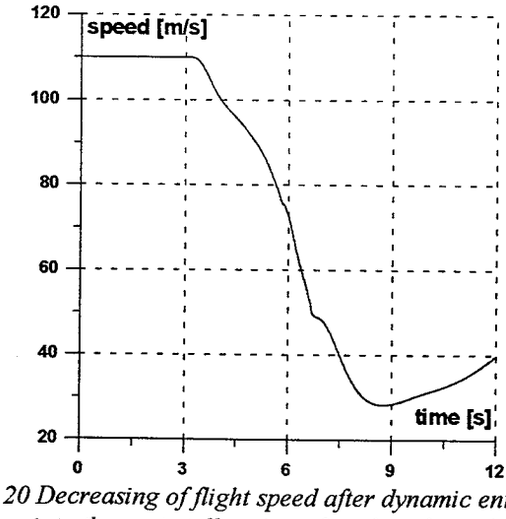

Fig.20 Decreasing of flight speed after dynamic entrance into the post-stall region of angles of attack

Copyright © 1998, by the International Council of the Aeronautical Sciences (ICAS)
and the American Institute of Aeronautics and Astronautics, Inc.

Fig.21 presents a comparison of transient angle of attack obtained by the aircraft depending on the centre of gravity position. Typical relations between the time to obtain high angle of attack, stability margin and current angle of attack are presented in[2] (see Fig.13 in[2]). Curves shown here in Fig.21 are even more rapidly-changing comparing to these given by Samoylovith. However, the common feature of both transient responses is the fact that stable aircraft can not go into the post-stall region of angles of attack. However, even a slightly unstable aircraft is able to reach the post-stall region very quickly.

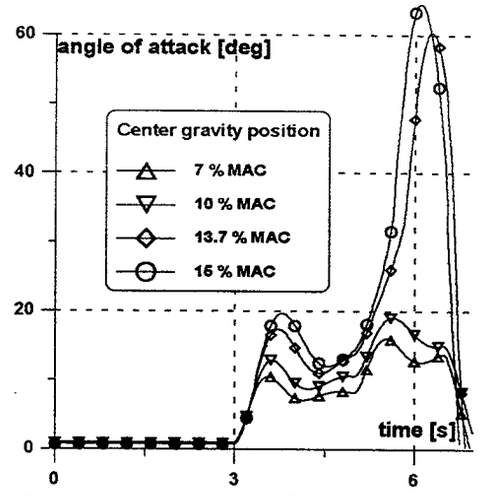

Fig.21 Increasing of angle of attack after dynamic entrance into the post-stall region for different position of the center of gravity

Conclusions

The combat value of post-stall manoeuvring as an air-to-air tactic remain a matter of controversy. According to Samoylovith Cobra manoeuvre is very impressive and can attract spectators at the air shows, but does not have any tactical significance. However, the somersault manoeuvre[3] is regarded as that of great combat importance in dog-fight. Lesson learned from the present investigations are as follows:

- aerodynamic characteristics necessary to perform numerical simulations in the post-stall region should be given in extended range of angle of attach (from 0° to 90°);
- transient responses of an aircraft are very sensitive to the centre of mass position and tailplane control function;
- trim parameters should be found before the dynamic equation of motion are numerically integrated. These parameters could be found either from the full nonlinear equations of the state of equilibrium or from simplified, two different sets of linnear equations;
- trim parameters in the below-stall and post-stall regions are continuos with respect to speed and angle of attack, however the solution in the transient range (about 30°) does not have any practical meaning.

References

1. W.Herbst, Dynamics of Air Combat, J.Aircraft, Vol.20, No.7, July 1983, pp.594-598.
2. O.Samoilovitch, Aerodynamic Configurations of Contemporary and Prospective Fighters, Proc.of Second Seminar on „Recent Research and Design Progress on Aeronautical Engineering and its Influence on Education", edited by Z.Goraj, Warsaw, Nov. 1996, part II, pp.233-246.
3. J.Rom, High Angle of Attack Aerodynamics - the State of Art and Future Challenges, Proceedings of Second Seminar on „Recent Research and Design Progress in Aeronautical Engineering and its Influence on Education" , edited by Z.Goraj, Warsaw 1997, Part I, pp.41-54.
4. Z.Goraj, New Directions of Research in Aeronautical Engineering - Breaking the Barriers, J.Theor.Appl.Mech., 4, 35, 1997, pp.781-812.
5. C.Alcorn, M.Croom, M.Francis, H.Ross, The X-31 Aircraft: Advances in Aircraft Agility and Performance, Prog. Aerospace Sci., Vol.32, pp.377-413, 1996.
6. R.Whitford, Fundamentals of Fighter Design, Cycle 6 papers in Air International, 1996-97.
7. J.M.Delery, Aspects of Vortex Breakdown, Prog.Aerospace Sci., 30, 1994, pp.1-59.
8. J.Lopez, Axisymmetric Vortex Breakdown, J.Fluid Mech., (1990), Vol.221, Part 1. Confined Swirling Flow: pp.533-552, Part 2. Physical Mechanisms: pp.553-576.
9. M.Boffadossi, Calculation of Vortex Breakdown over Delta Wing by a Vortex-Lattice Method, ICAS Proc. of 20th Congress, Sorrento, Sept.1996, pp.1201-1210.
10. B.A.Robinson, R.M.Barnett, S.Agrawal, Simple Numerical Criterion for Vortex Breakdown, AIAA Journal, Vol.32, No.1, 1994, pp.116-122.
11. I.Gursul, Criteria for Location of Vortex Breakdown over Delta Wings, Aeronautical Journal, May 1995, pp.194-196.
12. J.Luckring, Aerodynamics of Strake-Wing Interaction, Journ.of Aircraft, Vol.16, No.11, Nov.1979, pp.756-762.
13. E.Vizel, A.Gontchar, Investigations of Aerodynamic Characteristics of Part-Scale Aircraft Model of Moderate Wing Sweep Angle and the Structure of Vortices versus the LEX's Form-in Plane and its Parameters, (In Russian), Journ.-Technika Vojennogo Flota, No 1-2, 1994, pp.52-58.
14. Yu Dzelnin, Aircraft Stability and Maneuverability During Dynamic Departure at High Angles of Attack (In Russian), Journal - Technika Vojennogo Flota (ТВФ), No 1-2, 1994, pp.59-66.

Copyright © 1998, by the International Council of the Aeronautical Sciences (ICAS)
and the American Institute of Aeronautics and Astronautics, Inc.

15. L.Ericsson, Challenges in High-Alpha Vehicle Dynamics, Prog. Aerospace Sci., Vol.31, pp.291-334, 1995.
16. L.Ericsson, H.King, Rapid Prediction of High-Alpha Unsteady Aerodynamics of Slender-Wing Aircraft, Journ.of Aircraft, Vol.29, No.1, Jan.-Feb.1992, pp.85-92.
17. L.Ericsson, Pitch Rate Effects on Delta Wing Vortex Breakdown, Vol.33, No.3, May-June 1996, pp.639-642.
18. L.Ericsson, Delta Wing Vortex Breakdown Dynamics, AIAA Paper 95-0367, Jan.1995.
19. A.Khrabrov, K.Kolinko, Experimental Investigations of the High Aspect Ratio Wing Unsteady Aerodynamics at Stall Regimes and its Mathematical Modeling, Proceedings of Second Seminar on „Recent Research and Design Progress in Aeronautical Engineering and its Influence on Education" , edited by Z.Goraj, Warsaw 1997, Part I, pp. 195-200.
20. A.Khrabrov, O.Miatov, Experimental and Theoretical Investigations of Delta Wing High Angles of Attack Unsteady Aerodynamics, Proceedings of Second Seminar on „Recent Research and Design Progress in Aeronautical Engineering and its Influence on Education" , edited by Z.Goraj, Warsaw 1997, Part I, pp. 201-206.
21. Asselin M., An Introduction to Aircraft Performance, AIAA Education Series, Reston 1997.
22. G.Norris, Breaking the Stall Barrier, Flight International, 11-17 Nov.1992, pp.34-37.
23. Orlik-Rückemann, Dynamic Stability Testing of Aircraft - Needs Versus Capabilities, Prog.Aerospace Sci., Vol.16, No.4, 1975, pp.431-447.
24. Orlik-Rückemann, Aerodynamic Aspects of Aircraft Dynamics at High Angles of Attack, Jour.of Aircraft, Vol.20, No.9, Sept.1983, pp.737-752.
25. K.Orlik-Rückemann, Aerodynamic Coupling between Lateral and Longitudinal Degrees of Freedom, AIAA Journal, Vol.15, No.12, Dec.1977, pp.1792-1799.
26. A.A.Ghmmam, Z.Goraj, A Review of the Influence of High Angle of Attack Aerodynamics on Aircraft Dynamic Stability, Jour.Ther.Appl.Mech., 3, 33, 1995, pp.667-686.
27. K.H.Well, B.Faber, E.Berger, Maneuver Optimization of Aircraft Utilizing High Angles of Attack, ICAS Proceedings, 80-6.4., pp.257-264, 1980.
28. R.Whitford, Design for Air Combat, Jane's Publishing Company Limited, 1987.
29. K.Orlik-Rückemann, Aerodynamics of Manoeuvring Aircraft, Canadian Aeronautics and Space Journal, Vol.38, No.3, Sept.1992, pp.106-115.
30. D.Manor, W.Wentz Jr., Flow over Double-Delta Wing and Wing Body at High α, Jour.of Aircraft, Vol.22, No.1, Jan.1985, pp.78-82.
31. E.L.Tu, Vortex-Wing Interaction of a Close-Coupled Canard Configuration, Jour.of Aircraft, Vol.31, No.2, March-April 1994, pp.314-321.
32. M.E.Beyers, Interpretation of Experimental High-Alfa Aerodynamics - Implications for Flight Prediction, Jour. of Aircraft, Vol.32, No.2, March-April 1995, pp.247-261.
33. M.Beyers, Investigation of High-Manoeuvrability Flight Vehicle Dynamics, ICAS Proceedings, 80-7.2., pp.278-292, 1980.
34. H.John, W.Kraus, High Angle of Attack Characteristics of Different Fighter Configurations, AGARD-CP-247, Paper 2(15), 1979
35. J.Rom, High Angle of Attack Aerodynamics; Subsonic, Transonic, and Supersonic Flows, Springer-Verlag, New York 1992. Week & Space Technology, Aug.8, 1994, p.54.
36. Chambers J.R.,Overview of Stall/Spin Technology, AIAA Paper 80-1580, Danvers Aug.1980.
37. Goraj Z., Aerodynamics For High AOA And Introduction Of Polish Aviation Study, Proceedings of The 35th Aircraft Symposium, Tokyo 1997, pp.177-180.
38. E.L.Tu, Effect of Canard Deflection on Close-Coupled Canard-Wing-Body Aerodynamics, Jour.of Aircraft, Vol.31, No.1, Jan.-Feb. 1994, pp.138-145.
39. D.Hummel, H.Oelker, Effects of Canard Position on Aerodynamic Characteristics of a Close-Coupled Canard Configuration at Low Speed, Z.Flugwiss.Weltraumforsch.15 (1991) 74-88, pp.74-88.
40. Kendall E.R., Learjet G., The Minimum Induced Drag, Longitudinal Trim and Static Longitudinal Stability of Two-Surface and Three-Surface Airplanes, AIAA-84-2164.
41. L.Ericsson, Cobra Maneuver Unsteady Aerodynamic Considerations, Jour.of Aircraft, Vol.32., No.1, pp.214-216.
42. S.Ransom, Configuration Development of a Research Aircraft with Post-Stall Manoeuvrability, J.Aircraft, Vol.20, No.7, July 1983, pp.599-605.
43. R.Gütter, H.Friehmelt, R.Haiplik, Tactical Utility of the X-31A Using Post Stall Technologies, ICAS Proceedings, 96-3.7.5., pp.1574-1583, Sorento 1996.
44. Z.Dżygadło, G.Kowaleczko, K.Sybilski, Method of Control of a Straked Wing Aircraft for Cobra Manoeuvres, ICAS Proceedings, 96-3.7.4., pp.1566-1573, Sorento 1996.
45. Grafton S.B., Libbey Ch.E., Dynamic Stability Derivatives of a Twin-Jet Fighter model for Angles of Attack from -10° to 110° , NASA TN D-6091, Washington Jan.1971.
46. Grafton S.B., Anglin E.L., Dynamic Stability Derivatives at Angle of Attack from -5° to 90° for the Variable-Sweep Fighter Configuration with Twin Vertical Tails, NASA TN D-6909, Washington Oct.1972.

20203 II